

# Updated CMB, X- and $\gamma$ -ray constraints on majoron dark matter

Massimiliano Lattanzi,<sup>1,\*</sup> Signe Riemer-Sørensen,<sup>2</sup> Mariam Tórtola,<sup>3</sup> and J. W. F. Valle<sup>3,†</sup>

<sup>1</sup>*Dipartimento di Fisica e Science della Terra, Università di Ferrara and INFN, sezione di Ferrara, Polo Scientifico e Tecnologico - Edificio C Via Saragat, 1, I-44122 Ferrara Italy*

<sup>2</sup>*School of Mathematics and Physics, University of Queensland, St Lucia, Brisbane 4072, Queensland, Australia*

<sup>3</sup>*AHEP Group, Instituto de Física Corpuscular – C.S.I.C./Universitat de València*

*Campus de Paterna, Apt 22085, E-46071 València, Spain*

The majoron provides an attractive dark matter candidate, directly associated to the mechanism responsible for spontaneous neutrino mass generation within the standard model  $SU(3)_c \otimes SU(2)_L \otimes U(1)_Y$  framework. Here we update the cosmological and astrophysical constraints on majoron dark matter coming from Cosmic Microwave Background (CMB) and a variety of X- and  $\gamma$ -ray observations.

PACS numbers: 98.80.Es, 98.80.Jk, 95.30.Sf

## I. INTRODUCTION

It is by now established that only a small fraction (less than 20%) of the matter in the Universe is in the form of ordinary - i.e., baryonic - matter, while the rest is in the form of so-called “dark matter”. The existence of dark matter is inferred by gravitational anomalies at very different scales, ranging from galactic scales to cluster scales, and all the way up to the cosmological scales. In particular, the 9-year data from the Wilkinson Microwave Anisotropy Probe (WMAP) [1, 2] have provided even stronger support to the six-parameter  $\Lambda$ CDM model, although small-scale experiments like the Atacama Cosmology Telescope (ACT) [3] and the South Pole Telescope (SPT) [4] hint to interesting, albeit discordant, deviations from this simple picture, like e.g. the presence of other relativistic degrees of freedom, in addition to the standard model neutrinos, or deviations from ordinary gravity [5, 6]. On the other hand, the newly published results from the Planck satellite have provided an even stronger support to the minimal  $\Lambda$ CDM model [7].

If the  $\Lambda$ CDM model is certainly a phenomenological success, nevertheless it is puzzling from the theoretical point of view in many aspects. On one side, the nature of both dark matter and dark energy, that together make up for more than 95% of the total energy budget of the Universe, is still unknown. On the other side, the theory of inflation, that explains the formation of the primeval seeds for density fluctuations from which galaxies originate, is still waiting to be embedded in a more

fundamental theory. All these puzzles hint, and possibly have their solution in, some physics beyond the standard model (SM) of particle physics, or maybe in some modification of general relativity.

Although its precise nature is still unknown, there is no shortage of candidates for the role of dark matter. One of the most widely studied candidates to date is the supersymmetric neutralino. Recent results from the Large Hadron Collider (LHC), however, have greatly reduced the available parameter space for supersymmetry, at least in its simplest minimal supergravity implementations [8], reducing, perhaps, the appeal of supersymmetric dark matter candidates. Other possible candidates include axions, Kaluza-Klein dark matter, keV dark matter, such as sterile neutrinos, and many others. In particular, dark matter in the keV range has been advocated by many authors (see for example Refs. [9–11] and references therein) as a possible solution for the shortcomings of the cold dark matter scenario at small scales.

The evidence for the existence of dark matter is very strong, but only limited to effects related to its gravitational interaction. The search for non-gravitational evidence of the dark matter continues, in the form of direct and indirect detection experiments, and by looking for dark matter production in accelerators like the LHC. A precise underpinning of the dark matter and determination of its properties can only come through a combination of these approaches.

If the dark matter has any connection to the world of SM particles, there will be astrophysical signals one can search for, in particular high energy photons from annihilating or decaying dark matter (see Refs. [12, 13] for a recent review). The most studied scenarios are

\* lattanzi@fe.infn.it

† <http://astroparticles.ific.uv.es/>

the broad spectrum annihilation signals from neutralinos, but the real smoking gun is line emission (either directly from the decay/annihilation [14, 15] or from internal bremsstrahlung [16, 17]), for which the spectral and spatial distribution is not easily mimicked by astrophysical sources. The recent claim of line emission at  $E_\gamma = 130$  GeV in the Fermi data [18, 19] has spurred a renewed interest in emission line searches at high energy. However, the origin of the possible signal at  $E_\gamma = 130$  GeV is still unknown and caution is encouraged with respect to its interpretation [20].

It has been long suggested that the origin of dark matter could be related to the origin of neutrino masses [21, 22]. In fact, the smallness of neutrino masses, as compared to the other SM particles, is puzzling in itself. Most likely it is associated to the properties of the messenger states whose exchange is responsible for inducing them. This is the idea underlying the so-called seesaw mechanism [23–27], whose details remain fairly elusive. Especially appealing is the possibility that neutrino masses arise from the spontaneous violation of ungauged lepton number [28, 29]. The associated Nambu-Goldstone boson, the majoron, could acquire a mass from non-perturbative gravitational effects [30, 31], and play the role of the dark matter particle. In Ref. [32] the viability of the majoron as a dark matter particle was explored using the WMAP 3-year data and in Ref. [33] the possible X-ray signature associated to majoron decay was investigated. A specific theoretical model implementing the seesaw mechanism and an  $A_4$  flavour symmetry was described in [34].

In this paper, we update our previous constraints in the light of the more recent cosmological and astrophysical data. Regarding cosmology we use the WMAP 9-year data [1, 2] (as discussed in Sec. III, we do not expect our results to change significantly using other CMB data). On the astrophysical front we include emission line searches on the entire range of photon energies between 0.07 keV and 200 GeV from *Chandra* X-ray Observatory, X-ray Multi-Mirror Mission - Newton (*XMM*), High Energy Astronomy Observatory Program (*HEAO*), International Gamma-Ray Astrophysics Laboratory (*INTEGRAL*), Compton Gamma Ray Observatory (*CGRO*), and the Fermi Gamma-ray Space Telescope.

The paper is organized as follows. In Sec. II, we briefly recall the relevant majoron physics. In Secs. III and IV, we derive observational constraints on the majoron decay to neutrinos and photons, respectively, and we compare

them to the predictions of a general seesaw model. Finally, in Sec. V we draw our conclusions.

## II. SEESAW MAJORON PHYSICS

The basic idea of majoron physics is that the lepton number symmetry of the standard  $SU(3)_c \otimes SU(2)_L \otimes U(1)_Y$  model is promoted to a spontaneously broken symmetry [28, 29]. This requires the presence of a lepton-number-carrying complex scalar singlet,  $\sigma$ , coupling to the singlet neutrinos  $\nu_L^c$ , as follows,

$$\lambda \sigma \nu_L^c T \sigma_2 \nu_L^c + H.c. \quad (1)$$

with the Yukawa coupling  $\lambda$ . This term provides the large mass term in the seesaw mass matrix

$$\mathcal{M}_\nu = \begin{bmatrix} Y_3 v_3 & Y_\nu v_2 \\ Y_\nu^T v_2 & Y_1 v_1 \end{bmatrix} \quad (2)$$

in the basis of “left” and “right”-handed neutrinos  $\nu_L$ ,  $\nu_L^c$ . The model is characterized by singlet, doublet and triplet Higgs scalars whose vacuum expectation values (vevs) are arranged to satisfy  $v_1 \gg v_2 \gg v_3$  obeying a simple vev seesaw relation of the type

$$v_3 v_1 \sim v_2^2. \quad (3)$$

The vev  $v_1$  drives lepton number violation and induces also a small but nonzero  $v_3$ , while  $v_2$  is fixed by the masses of the weak gauge bosons, the  $W$  and the  $Z$ . Note that the vev seesaw condition implies that the triplet vev  $v_3 \rightarrow 0$  as the singlet vev  $v_1 \rightarrow \infty$ . The three vevs determine all entries in the seesaw neutrino mass matrix. Regarding the Yukawa couplings,  $Y_\nu$  is an arbitrary flavour matrix, while  $Y_3$  and  $Y_1$  are symmetric. The effective light neutrino mass obtained by perturbative diagonalization of Eq. (2) is of the form

$$m_\nu \simeq Y_3 v_3 - Y_\nu Y_1^{-1} Y_\nu^T \frac{v_2^2}{v_1} \quad (4)$$

Together with Eq. (3) this summarizes the essence of the seesaw mechanism.

In order to identify which combination of Higgs fields gives the majoron,  $J$ , one may write the scalar potential explicitly, minimize it, and determine the resulting scalar mass matrices. However, one can do this simply by exploiting the invariance properties of the Higgs potential  $V$  [29]. The result is proportional to the combination

$$J \propto v_3 v_2^2 \text{Im}(\Delta^0) - 2v_2 v_3^2 \text{Im}(\Phi^0) \quad (5)$$

$$+ v_1 (v_2^2 + 4v_3^2) \text{Im}(\sigma) \quad (6)$$

up to a normalization factor.  $\text{Im}()$  denotes the imaginary parts, while  $\Delta^0$  and  $\Phi^0$  refer to the neutral components of the triplet and doublet scalars respectively, and  $\sigma$  is the scalar singlet introduced in Eq. 1. We remark the presence of the quartic lepton-number-conserving term

$$\Phi^\dagger \Delta \tau_2 \Phi^* \sigma^* + H.c. \quad (7)$$

in the scalar potential. Here  $\tau_2$  is the weak isospin Pauli matrix, and  $v_2 \equiv \langle \Phi \rangle$ ,  $v_1 \equiv \langle \sigma \rangle$ ,  $v_3 \equiv \langle \Delta \rangle$ . This term illustrates the need for mixing among neutral fields belonging to all three Higgs multiplets in the expression for the majoron, Eq. (5). As a result the majoron has an explicit coupling to two photons leading to a possible indirect detection of majoron dark matter by searching for the corresponding high energy photons [33], which we treat in Sec. IV.

We now turn to the form of the couplings of the majoron within the above seesaw scheme, characterized by spontaneous lepton number violation in the presence of singlet, doublet and triplet Higgs scalars. Again one can derive the form of the couplings of the majoron using only the symmetry properties, as described in Ref. [29],

$$\mathcal{L}_{\text{Yuk}} = \frac{iJ}{2} \sum_{ij} \nu_i^T g_{ij} \sigma_2 \nu_j + H.c. \quad (8)$$

The result is a perturbative expansion for the majoron couplings

$$g_{ij} = -\frac{m_i^\nu}{v_1} \delta_{ij} + \dots \quad (9)$$

where the dots  $\dots$  denote higher order terms. One sees that, to first approximation, the majoron couples to the light mass-eigenstate neutrinos inversely proportional to the lepton number violation scale  $v_1 \equiv \langle \sigma \rangle$  and proportionally to their mass. With this we can compute the dark matter majoron decay rate to neutrinos as

$$\Gamma_{J \rightarrow \nu\nu} = \frac{m_J}{32\pi} \frac{\sum_i (m_i^\nu)^2}{2v_1^2}, \quad (10)$$

where the Majoron mass  $m_J$  is presumably generated by non-perturbative gravitational effects [30, 31]. Moreover, there is a sub-leading majoron decay mode to photons. Within the general seesaw model this decay is induced at the loop level, resulting in [33]

$$\Gamma_{J \rightarrow \gamma\gamma} = \frac{\alpha^2 m_J^3}{64\pi^3} \left| \sum_f N_f Q_f^2 \frac{2v_3^2}{v_2^2 v_1} (-2T_3^f) \frac{m_J^2}{12m_f^2} \right|^2, \quad (11)$$

where  $N_f$ ,  $Q_f$ ,  $T_3^f$  and  $m_f$  denote respectively the color factor, electric charge, weak isospin and mass of the SM

electrically charged fermions  $f$ . We note that this formula is an approximation valid for  $m_J \ll m_f$ ; however we will always use the exact formula in the actual calculations.

The decay of the majoron dark matter to neutrinos provides the most essential and model-independent feature of the majoron dark matter scenario, namely, it is a decaying dark matter model where the majoron decays mainly to neutrinos, a mode that is constrained from the CMB observations, as we discuss in Sec. III.

### III. CMB CONSTRAINTS ON THE INVISIBLE DECAY $J \rightarrow \nu\nu$

#### A. Method

We start by deriving constraints on the majoron properties from CMB anisotropy data. The majoron differs from most dark matter candidates in that it is unstable, since it must decay to neutrinos, as seen in Eq. (10), although it obviously has to be long-lived enough to play the role of the dark matter today.

In order to investigate the observable effects of majoron decay on the CMB, the Boltzmann equation describing the phase-space evolution of dark matter particles must be modified accordingly, as shown e.g. in Ref. [35], both at the background and at the perturbation level. The main effect of the late dark matter decay to invisible relativistic particles is an increase of the late integrated Sachs-Wolfe effect, caused by the presence of an extra radiation component at small redshifts. This is reflected in the CMB power spectrum by an increased amount of power at the largest angular scales (i.e., small multipoles). Too large a decay rate would produce too much radiation and too much large-scale power, and thus be at variance with observations. In Ref. [32] two of us have used this effect to constrain the majoron lifetime. However, we did not take properly into account the effect of majoron decay on the age of the Universe; this led to an underestimate of the upper limit of the majoron decay rate. We have now corrected this.

We use a modified version of CAMB [36], taking into account the finite lifetime of the majoron, to evolve the cosmological perturbations and compute the anisotropy spectrum of the CMB for given values of the cosmological parameters. We assume that we can neglect the velocity dispersion of majorons, i.e. we treat the majoron as a cold dark matter particle ( $m_J \gg T_J$ ). In

order to compute bayesian confidence intervals and sample the posterior distributions for the parameters of the model, given some data, we use the Metropolis-Hastings algorithm as implemented in CosmoMC [37] (interfaced with our modified version of CAMB). The model can be completely characterized by the six parameters of the standard  $\Lambda$ CDM model, namely the present density parameters  $\Omega_b h^2$  and  $\Omega_{\text{dm}} h^2$  of baryons and dark matter respectively, the angular size of the sound horizon at recombination<sup>1</sup>  $\theta$ , the optical depth to recombination  $\tau_{\text{rec}}$ , the spectral index  $n_s$  and amplitude  $A_s$  (evaluated at the pivot scale  $k_0 = 0.002 \text{ Mpc}^{-1}$ ) of the spectrum of primordial scalar fluctuations, to which we add the decay rate  $\Gamma_{J \rightarrow \nu\nu}$  of majorons to neutrinos. We marginalize over the amplitude of the contamination from the Sunyaev-Zel'dovich signal. We assume spatial flatness, massless neutrinos and adiabatic initial conditions.

Following our previous work [32], instead of  $\Omega_{\text{dm}} h^2$  we use, as a base parameter, the quantity  $s_{\text{early}}$  defined as:

$$s_{\text{early}} \equiv \left. \frac{\rho_{\text{dm}}}{\rho_{\text{b}}} \right|_{t \ll \Gamma_{J \rightarrow \nu\nu}^{-1}}, \quad (12)$$

*i.e.*, the ratio between the energy densities of dark matter and baryons at early times. This can be related to the present dark matter density by means of

$$\Omega_{\text{dm}} h^2 = s_{\text{early}} \Omega_b h^2 e^{-\Gamma_{J \rightarrow \nu\nu}^{-1} t_0}, \quad (13)$$

where  $t_0$  is the present age of the Universe. Also, we do not vary directly the decay rate  $\Gamma_{J \rightarrow \nu\nu}$  in our Monte Carlo runs, but instead the ratio  $\Gamma_{J \rightarrow \nu\nu}/H_0$ . Finally, we express the amplitude of primordial fluctuations in terms of  $\ln(10^{10} A_s)$ . Our base parameter set, consisting of those parameters with uniform priors that are varied in the Monte Carlo runs, is summarized in the upper part of Tab. I.

We perform our analysis using the most recent WMAP 9-year temperature and polarization data [1, 2]. In particular, for the temperature power spectrum we include data up to  $\ell_{\text{max}} = 1200$ . We use the latest (V5) version of the WMAP likelihood code, publicly available at the lambda website<sup>2</sup>.

<sup>1</sup> We have also repeated our analysis using  $H_0$  as a base parameter in place of  $\theta$  and found excellent agreement between the results obtained using the two parameterizations.

<sup>2</sup> <http://lambda.gsfc.nasa.gov/>

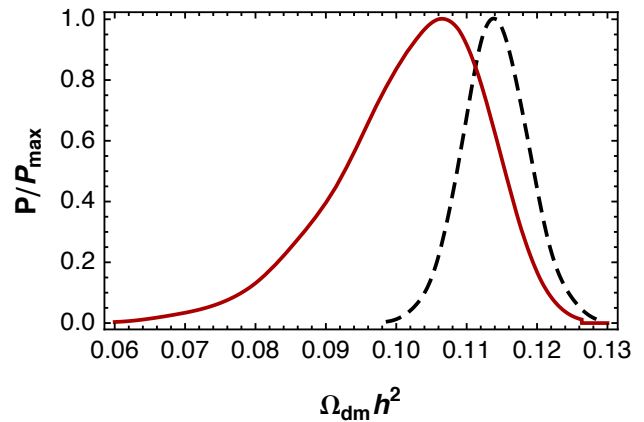


**FIG. 1.** One-dimensional posterior for the dark matter density parameter  $\Omega_{\text{dm}} h^2$  obtained from the WMAP9 data, for the  $\Lambda$ CDM (black dashed) and decaying majoron DM (red solid) models.

## B. Results

We first perform a control  $\Lambda$ CDM run by fixing the value of  $\Gamma_{J \rightarrow \nu\nu}$  to 0 (*i.e.*, we consider stable dark matter) and check that we can consistently reproduce the results quoted in the WMAP9 parameter paper [1]. Then we allow for the possibility of decaying dark matter; our results for the cosmological parameters are summarized in the fourth column of Tab. I. We find that the limits on the parameters of the standard  $\Lambda$ CDM model do not change significantly, with the one exception of the present dark matter density. In particular, taking as a reference the values quoted in Table 3 of Ref. [1], the uncertainties of the other parameters increase by less than 10%, and the posterior means shift by a fraction of a standard deviation at most.

For the present majoron density parameter, we find:

$$\Omega_{\text{dm}} h^2 = 0.102 \pm 0.010 \quad (68\% \text{ C.L.}). \quad (14)$$

Compared with the WMAP9  $\Lambda$ CDM result of  $\Omega_{\text{dm}} h^2 = 0.1138 \pm 0.0045$  [1], our estimate is shifted towards smaller values, and has an uncertainty which is a factor two larger. In Fig. 1, we compare the marginalized one-dimensional posterior for  $\Omega_{\text{dm}} h^2$  in the framework of the decaying dark matter model, with the one obtained from our control  $\Lambda$ CDM run. The reason for both the shift and the increase of the error bars will be discussed below.

For the purpose of the present analysis, we are mainly interested in the limits on the decay width of majoron to neutrinos,  $\Gamma_{J \rightarrow \nu\nu}$ . We get the following upper limit at

**TABLE I.** Cosmological parameter used in the analysis. The upper part of the table lists the base parameters, *i.e.*, those with uniform priors that are varied in the Monte Carlo run. The lower part lists derived parameters of interest. For each parameter, we quote the initial prior range (for base parameters only) and the confidence limits, in the form of posterior mean  $\pm$  68% uncertainty, with the exception of those parameter for which we can only derive an upper limit. In this case we only report the 95% confidence limit.

Parameter	Definition	Prior range	Limits
$\Omega_b h^2$	Present density of baryons	[0.005, 0.1]	$0.02290 \pm 0.00054$
$s_{\text{early}}$	Primordial dark matter to baryon ratio <sup>a</sup>	[0, 10]	$4.92 \pm 0.27$
$100\theta$	$100 \times$ angular size of the sound horizon at recombination	[0.5, 10]	$1.0401 \pm 0.0023$
$\tau_{\text{rec}}$	Optical depth to recombination	[0.01, 0.8]	$0.090 \pm 0.014$
$n_s$	Spectral index of scalar perturbations	[0.5, 1.5]	$0.977 \pm 0.014$
$\ln(10^{10} A_s)$	Log amplitude of scalar perturbations at $k_0 = 0.002 \text{ Mpc}^{-1}$	[2.7, 4.0]	$3.162 \pm 0.048$
$\Gamma_{J \rightarrow \nu\nu} H_0^{-1}$	Ratio between majoron decay rate and expansion rate	[0, 1]	$< 0.269$
$\Omega_{\text{dm}} h^2$	Present dark matter density	...	$0.102 \pm 0.010$
$\Omega_\Lambda$	Present dark energy density <sup>b</sup>	...	$0.743 \pm 0.030$
$H_0$	Hubble parameter today ( $\text{km s}^{-1} \text{ Mpc}^{-1}$ )	...	$71.5 \pm 2.6$
$\Gamma_{J \rightarrow \nu\nu}$	Majoron decay rate to neutrinos ( $10^{-19} \text{ s}^{-1}$ )	...	$< 6.40$
$m_J^{\text{eff}}$	Effective majoron mass <sup>c</sup> (keV)	...	$0.1577 \pm 0.0067$

<sup>a</sup> See definition in Eq. (12).

<sup>b</sup> We consider a constant equation of state  $w = -1$ .

<sup>c</sup> See definition in the text.

95% C.L.

$$\Gamma_{J \rightarrow \nu\nu} \leq 6.4 \times 10^{-19} \text{ s}^{-1}. \quad (15)$$

after marginalizing over the remaining parameters of the model. This results in a lower limit to the majoron lifetime  $\tau_J \geq 50 \text{ Gyr}$ , roughly four times the age of the Universe. This limit is slightly relaxed to  $\tau_J \geq 37 \text{ Gyr}$  when we allow for the possibility of extra degrees of freedom at the time of recombination, by varying  $N_{\text{eff}}$ .

In the left panel of Fig. 2 we show 68% and 95% confidence regions in the  $(\Gamma_{J \rightarrow \nu\nu}, \Omega_{\text{dm}} h^2)$  parameter plane. There is an evident anti-correlation between decay rate and abundance that is explained by the fact, already discussed in Ref. [32], that the CMB anisotropy spectrum is mainly sensitive to the amount of dark matter prior to the time of recombination (through the height of the first peak), as this sets the time of matter-radiation equality. Once the amount of dark matter in the early Universe is fixed, increasing the decay rate results in a smaller amount of dark matter at the present time, and viceversa. This degeneracy between  $\Omega_{\text{dm}} h^2$  and  $\Gamma_{J \rightarrow \nu\nu}$  explains the different shape of the posteriors shown in Fig. 1, and consequently explains the lower value and larger uncertainty of the estimate of  $\Omega_{\text{dm}} h^2$  with respect to those obtained for  $\Lambda\text{CDM}$ . In fact, if we compute constraints on the *primordial* dark matter density (for example con-

sidering the combination  $\Omega_{\text{dm}} h^2 \exp(\Gamma_{J \rightarrow \nu\nu} t_0)$ , which is, up to a multiplicative constant, the comoving density of dark matter at early times), we find consistent results between the  $\Lambda\text{CDM}$  and the majoron DM models.

In the limit of cold dark matter, one can not directly constrain the mass of the dark matter particle itself, since this quantity never appears explicitly neither in the background nor in the perturbation equations. Instead, the mass only appears implicitly inside the physical density parameter  $\Omega_{\text{dm}} h^2$ , in combination with the present number density  $n_{\text{dm}}^0$ , since for nonrelativistic particles  $\Omega_{\text{dm}} h^2 \propto \rho_{\text{dm}} = m_{\text{dm}} n_{\text{dm}}^0$ . The calculation of the number density relies on the knowledge of the production mechanism of the dark matter particle and on its thermal history. If the majoron was in thermal equilibrium with the rest of the cosmological plasma at some early time, and decoupled while still relativistic, one finds

$$\Omega_{\text{dm}}^{\text{th}} h^2 = \left( \frac{g_{*S}}{106.75} \right)^{-1} \left( \frac{m_J}{1.40 \text{ keV}} \right) e^{\Gamma_{J \rightarrow \nu\nu} t_0}, \quad (16)$$

where  $g_{*S}$  parametrizes the entropy content of the Universe at the time of majoron decoupling. If the majoron decouples when all the degrees of freedom of the SM of particle physics are excited and in thermal equilibrium, one has  $g_{*S} = 106.75$ . In order to account for a more

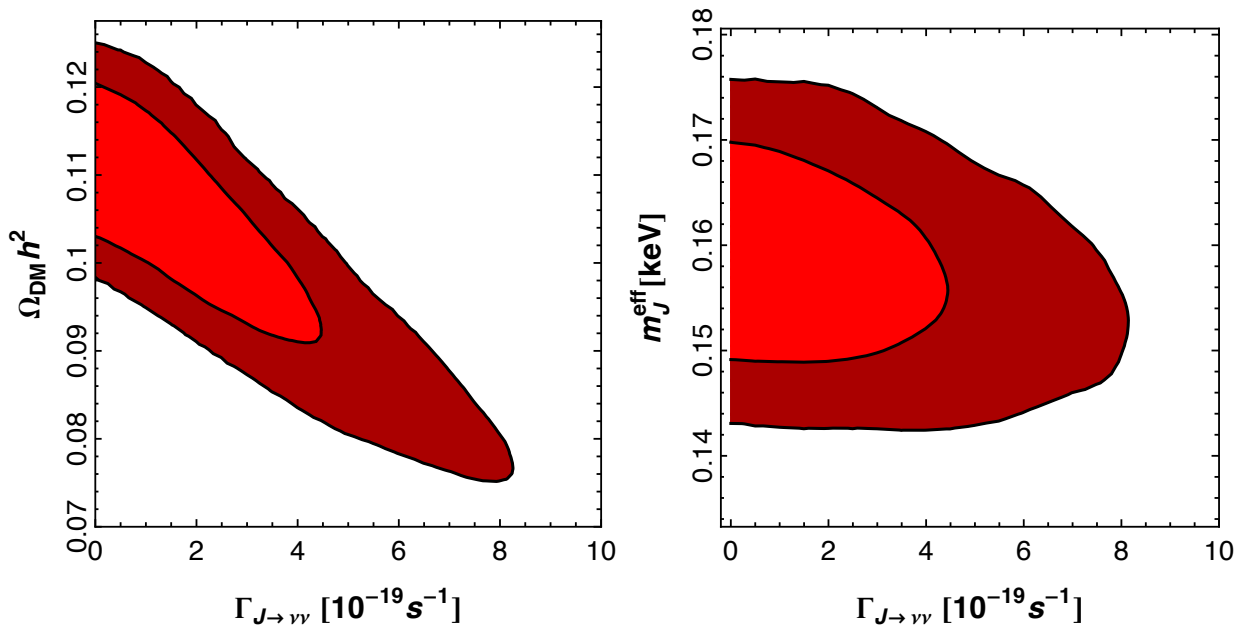


**FIG. 2.** Two-dimensional WMAP-9 constraints on the majoron dark matter parameters. The light (dark) shaded regions correspond to 68% (95%) confidence regions. Left panel: present density vs. decay rate to neutrinos. Right panel: effective mass vs. decay rate to neutrinos.

general scenario, following Ref. [32], we write

$$\Omega_{\text{dm}}^{\text{th}} h^2 = \beta \left( \frac{m_J}{1.40 \text{ keV}} \right) e^{\Gamma_{J \rightarrow \nu\nu} t_0}, \quad (17)$$

so that  $\beta = 1$  corresponds to the case of a thermal majoron decoupling when  $g_{*S} = 106.75$ . The parameter  $\beta$  encodes our ignorance about the majoron thermal history, and  $\beta \neq 1$  can account both for a thermal majoron decoupling when  $g_{*S} \neq 106.75$ , or for a non-thermal distribution. Non-thermal production mechanisms include, for example, a phase transition [22] or the evaporation of majoron strings [38]. However, a detailed study relating the parameters of the underlying particle physics model to the cosmological majoron abundance in any of these scenarios is still lacking, so it is difficult to identify, on purely theoretical grounds, the range of reasonable values of beta.

Using Eqs. (17), we can constrain the “effective mass”  $m_J^{\text{eff}} \equiv \beta m_J$  and get:

$$m_J^{\text{eff}} = (0.158 \pm 0.007) \text{ keV} \quad (68\% \text{ C.L.}). \quad (18)$$

In the right panel of Fig. 2 we show 68% and 95% confidence regions in the  $(\Gamma_{J \rightarrow \nu\nu}, m_J^{\text{eff}})$  plane. This should substitute the results appearing in Ref. [32]. Moreover, we stress again that this constraints can be read in terms of the actual majoron mass only in the case of thermal

majoron decoupling when  $g_{*S} = 106.75$  (i.e.,  $\beta = 1$ ). Since the CMB does not really constrain the majoron mass (at least in the cold limit), in the next section we will consider values of the mass also outside the keV range. We do not consider values of the mass below  $\sim 0.15$  eV (corresponding to  $\beta \gtrsim 1$ ) as they are likely to lead to problems in the context of structure formation due to the large free-streaming length of the particle [39] (although a detailed study would require the knowledge of the full distribution function). The soft X-ray band is also observationally challenging with no current high-resolution observations appropriate for line-searches.

#### IV. X- AND $\gamma$ -RAY CONSTRAINTS ON THE PHOTON DECAY $J \rightarrow \gamma\gamma$

One of the most interesting features of spontaneous lepton number violation within the general  $\text{SU}(3)_c \otimes \text{SU}(2)_L \otimes \text{U}(1)_Y$  seesaw model is that the neutrino decay mode in Eq. (10) is accompanied by a two-photon mode, Eq. (11), as a result of the Eq. (5). The decay into photons is constrained by a number of astrophysical observations.

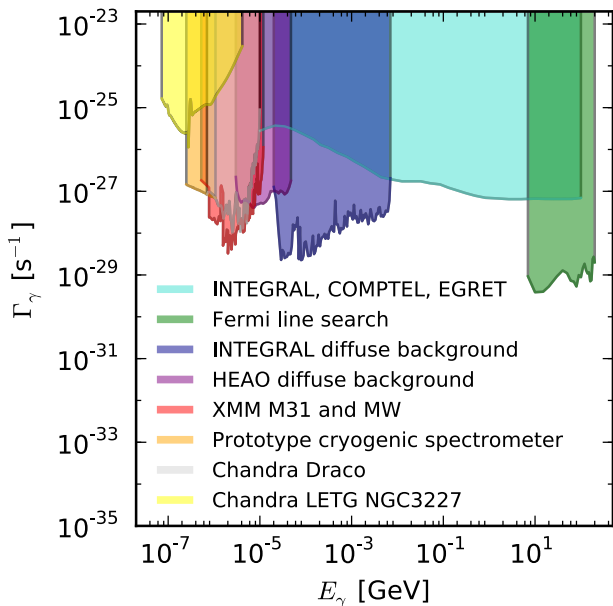


**FIG. 3.**  $3\sigma$  line emission constraints on the decay rate into two mono-energetic photons. These constraints apply to all dark matter candidates with this signature. The constraints are taken from: yellow [40], orange [41] (conservatively rescaled by a factor of two due to mass estimate uncertainties as recommended in [10]), red [42], grey [43], purple [44], blue [45], cyan [46], green [47].

#### A. Existing constraints

In Fig. 3 we plot the emission line constraints over the wide range of photon energies of 0.07 keV to 200 GeV.

The very soft X-ray emission is covered by *Chandra* Low Energy Transmission Grating (LETG) observations of NGC3227 (0.07 – 4.1 keV) [40] and a rocket borne light cryogenic spectrometer (0.25 – 1.1 keV) [41, 48].

The 0.3 – 12 keV range is well covered with constraints from various objects observed with the *Chandra* and *XMM* X-ray telescopes [42–45, 49–58]. In Fig. 3 we have chosen the strongest robust constraints<sup>3</sup> from *XMM* observations of the Milky Way and M31 [42] and from *Chandra* observations of the Draco dwarf galaxy [43].

<sup>3</sup> Some analyses have claimed stronger constraints in this energy interval, but were later found to be too optimistic. Ref. [59] underestimated the flux by two orders of magnitude [49, 51]. According to Ref. [42] the mass was overestimated in Ref. [60] leading to too restrictive constraints. The constraints in Ref. [61] might be too restrictive due to the choice of source profile [45], and the spectral resolution appears overestimated in Ref. [62]

The diffuse X-ray background observed with HEAO was searched for line emission by Ref. [44] over the range 3 – 48 keV, and line emission constraints have been derived from INTEGRAL SPI observations of the soft  $\gamma$ -ray background (20 keV – 7 MeV) [45]. For energies above those covered by INTEGRAL the constraints are two orders of magnitude worse as this range is only covered by a combination of the rather old COMPTEL and EGRET instruments onboard the CGRO. However, line emission constraints have been derived up to 100 GeV [46]. The most recent flagship for  $\gamma$ -ray searches is the Fermi  $\gamma$ -ray Space Telescope, for which line emission searches have been performed for the range of 7 – 200 GeV [47].

#### B. Future improvements

The constraints on the majoron decay rate into two mono-energetic photons shown in Fig. 3 can be improved by increasing the statistics or the spectral resolution. Increasing statistics (either by exposure time or by sensitivity) improves the constraints as  $\Gamma_{\gamma\gamma}^{\text{new}} = \sqrt{N_{\gamma\gamma}^{\text{ex}}/N_{\gamma\gamma}^{\text{new}}}\Gamma_{\gamma\gamma}^{\text{ex}}$ , where  $N_{\gamma\gamma}^{\text{ex,new}}$  are the existing and new total of photons per bin (assuming both source and background counts increase by the same amount). Increasing the spectral resolution improves the constraints directly as  $\Gamma_{\gamma\gamma}^{\text{new}} = E_{\text{FWHM}}^{\text{new}}/E_{\text{FWHM}}^{\text{ex}}\Gamma_{\gamma\gamma}^{\text{ex}}$  and is consequently preferable but also technically more challenging.

#### C. Model comparison

We now compare the observational constraints obtained in the previous section to the predictions of different realizations of a general majoron seesaw model. In particular, we perform a random scan over the Yukawa matrices ( $Y_\nu, Y_1, Y_3$ ) and vevs ( $v_1, v_3$ ) that characterize the seesaw mass matrix  $\mathcal{M}_\nu$  in Eq. (2). For each point in the parameter space we evaluate the effective light neutrino mass matrix and the Majoron decay rate to neutrinos following Eqs. (4) and (10), respectively. We then choose, among all possible realizations, those that are in agreement with current neutrino oscillation data [63] as well as with the bound on neutrino decay rate in Eq. (15). Finally we compute the corresponding decay rate to photons, as described in Sec. II.

We show the results of our scan in parameter space in Fig. 4, together with the constraints already shown in Fig. 3. It is clearly visible that the  $J \rightarrow \gamma\gamma$  con-

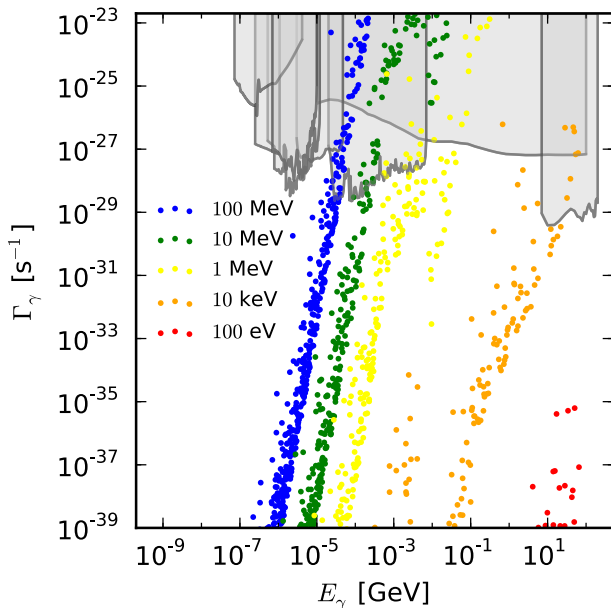


**FIG. 4.** The line emission constraints from Figure 3 (grey) compared to model predictions (colored dots), for different values of the triplet vev  $v_3$ .

straints from line emission searches already begin to cut the remaining parameter space for realistic models. This happens in particular for models with  $v_3$  larger than a few MeVs. However, models with lower values of the triplet vev predict a photon flux that falls below the observational limits, as seen from the figure. For example, for  $v_3 < 100$  eV, predictions lie below both current and planned  $\gamma$ -ray observatory sensitivities.

Note that, although for masses above 1 MeV the majoron could decay to electron-positron pairs, nevertheless the branching ratio is negligible. However, at even higher masses, new decay channels open up, with the production of muon-anti-muon pairs etc. In this case these decays would produce continuum gamma-ray emission at energies below the emission line. This does not change any of the constraints given in Figs. 3 and 4, though it would give rise to additional constraints from continuum photon fluxes and subsequent radio emission.

## V. CONCLUSIONS

We have updated previous constraints on the parameters of the majoron dark matter model using the most recent CMB, X- and  $\gamma$ -ray observations. From the CMB, we have derived an upper limit on the rate of the invisible decay of the dark matter particle, namely, in the framework of the model under consideration, on the majoron decay to neutrinos. Translated in terms of the particle lifetime, this constrains the majoron lifetime to be larger than 50 Gyrs.

Since, as already shown in Ref. [32], the late decay of dark matter mostly affects the large angular scale part of the CMB power spectrum, where the uncertainty is dominated by cosmic variance, we do not expect a dramatic improvement by using the Planck data rather than WMAP9. Likewise, the small-scale data from ACT and SPT are not expected to change significantly our constraints. However, we cannot exclude that a more precise determination of the intermediate to high-ell part of the spectrum could affect, via parameter degeneracies, the estimation of the decay rate. We defer a more careful study of this issue to a future work.

The majoron also possesses a subleading decay mode to two photons, that can be constrained by astrophysical observations in the X and  $\gamma$  regions. We have compared these limits to the theoretical predictions corresponding to different values for the parameters of the underlying particle physics model. We have found that the observational constraints already exclude part of the parameter space for models in which the vev of the triplet  $v_3$  is larger than a few MeVs. On the other hand, for smaller values of  $v_3$ , the current limits need to be improved by at least 6 orders of magnitude before the allowed region in parameter space can be reduced.

## VI. ACKNOWLEDGMENTS

Work supported by MINECO grants FPA2011-22975 and MULTIDARK Consolider CSD2009-00064, by Prometeo/2009/091 (Gen. Valenciana), by EU ITN UNILHC PITN-GA-2009-237920. The work of M.L. has been supported by Ministero dell’Istruzione, dell’Università e della Ricerca (MIUR) through the PRIN grant “Galactic and extragalactic polarized microwave emission” (contract number PRIN 2009XZ54H2-002). The work of M.T. is supported by CSIC under the JAE-Doc programme, co-funded by the European Social Fund.



- 
- [1] G. Hinshaw, D. Larson, E. Komatsu, D. Spergel, C. Bennett, *et al.*, (2012), arXiv:1212.5226 [astro-ph.CO].
- [2] C. Bennett, D. Larson, J. Weiland, N. Jarosik, G. Hinshaw, *et al.*, (2012), arXiv:1212.5225 [astro-ph.CO].
- [3] J. L. Sievers, R. A. Hlozek, M. R. Nolta, V. Acquaviva, G. E. Addison, *et al.*, (2013), arXiv:1301.0824 [astro-ph.CO].
- [4] Z. Hou, C. Reichardt, K. Story, B. Follin, R. Keisler, *et al.*, (2012), arXiv:1212.6267 [astro-ph.CO].
- [5] S. Riemer-Sørensen, D. Parkinson, T. M. Davis, and C. Blake, *Astrophys. J.* **763**, 89 (2013), arXiv:1210.2131 [astro-ph.CO].
- [6] S. Riemer-Sørensen, D. Parkinson, and T. M. Davis, *PASA* **30**, e029 (2013), arXiv:1301.7102 [astro-ph.CO].
- [7] P. Ade *et al.* (Planck Collaboration), (2013), arXiv:1303.5076 [astro-ph.CO].
- [8] S. Caron (ATLAS collaboration), (2011), arXiv:1106.1009 [hep-ex].
- [9] H. de Vega, M. Falvella, and N. Sanchez, (2012), arXiv:1203.3562 [astro-ph.CO].
- [10] A. Boyarsky, O. Ruchayskiy, and M. Shaposhnikov, *Annual Review of Nuclear and Particle Science* **59**, 191 (2009), arXiv:0901.0011 [hep-ph].
- [11] M. Drewes, *ArXiv e-prints* (2013), arXiv:1303.6912 [hep-ph].
- [12] T. Bringmann and C. Weniger, *Physics of the Dark Universe* **1**, 194 (2012), arXiv:1208.5481 [hep-ph].
- [13] A. Boyarsky, D. Iakubovskiy, and O. Ruchayskiy, *Physics of the Dark Universe* **1**, 136 (2012), arXiv:1306.4954 [astro-ph.CO].
- [14] L. Bergström and P. Ullio, *Nuclear Physics B* **504**, 27 (1997), arXiv:hep-ph/9706232.
- [15] Z. Bern, P. Gondolo, and M. Perelstein, *Physics Letters B* **411**, 86 (1997), arXiv:hep-ph/9706538.
- [16] J. F. Beacom, N. F. Bell, and G. Bertone, *Physical Review Letters* **94**, 171301 (2005), arXiv:astro-ph/0409403.
- [17] T. Bringmann, L. Bergström, and J. Edsjö, *Journal of High Energy Physics* **1**, 049 (2008), arXiv:0710.3169 [hep-ph].
- [18] T. Bringmann, X. Huang, A. Ibarra, S. Vogl, and C. Weniger, *JCAP* **7**, 054 (2012), arXiv:1203.1312 [hep-ph].
- [19] C. Weniger, *JCAP* **8**, 007 (2012), arXiv:1204.2797 [hep-ph].
- [20] A. Boyarsky, D. Malyshev, and O. Ruchayskiy, *ArXiv e-prints* (2012), arXiv:1205.4700 [astro-ph.HE].
- [21] G. Gelmini, D. N. Schramm, and J. W. F. Valle, *Phys. Lett.* **B146**, 311 (1984).
- [22] V. Berezhinsky and J. W. F. Valle, *Phys. Lett.* **B318**, 360 (1993), hep-ph/9309214.
- [23] M. Gell-Mann, P. Ramond, and R. Slansky, (1979), print-80-0576 (CERN).
- [24] T. Yanagida, (KEK lectures, 1979), ed. O. Sawada and A. Sugamoto (KEK, 1979).
- [25] R. N. Mohapatra and G. Senjanovic, *Phys.Rev.Lett.* **44**, 912 (1980).
- [26] J. Schechter and J. W. F. Valle, *Phys. Rev.* **D22**, 2227 (1980).
- [27] G. Lazarides, Q. Shafi, and C. Wetterich, *Nucl. Phys.* **B181**, 287 (1981).
- [28] Y. Chikashige, R. N. Mohapatra, and R. D. Peccei, *Phys. Lett.* **B98**, 265 (1981).
- [29] J. Schechter and J. W. F. Valle, *Phys. Rev.* **D25**, 774 (1982).
- [30] S. R. Coleman, *Nucl. Phys.* **B310**, 643 (1988).
- [31] R. Kallosh, A. D. Linde, D. A. Linde, and L. Susskind, *Phys. Rev.* **D52**, 912 (1995), arXiv:hep-th/9502069.
- [32] M. Lattanzi and J. W. F. Valle, *Phys. Rev. Lett.* **99**, 121301 (2007), arXiv:0705.2406 [astro-ph].
- [33] F. Bazzocchi *et al.*, *JCAP* **0808**, 013 (2008), arXiv:0805.2372 [astro-ph].
- [34] J. Esteves, F. Joaquim, A. Jshipura, J. Romao, M. Tortola, *et al.*, *Phys.Rev.* **D82**, 073008 (2010), arXiv:1007.0898 [hep-ph].
- [35] M. Kaplinghat, R. E. Lopez, S. Dodelson, and R. J. Scherrer, *Phys. Rev.* **D60**, 123508 (1999), astro-ph/9907388.
- [36] A. Lewis, A. Challinor, and A. Lasenby, *Astrophys. J.* **538**, 473 (2000), astro-ph/9911177.
- [37] A. Lewis and S. Bridle, *Phys. Rev.* **D66**, 103511 (2002), astro-ph/0205436.
- [38] I. Rothstein, K. Babu, and D. Seckel, *Nucl.Phys.* **B403**, 725 (1993), arXiv:hep-ph/9301213 [hep-ph].
- [39] A. Boyarsky, J. Lesgourgues, O. Ruchayskiy, and M. Viel, *JCAP* **0905**, 012 (2009), arXiv:0812.0010 [astro-ph].
- [40] F. Bazzocchi, M. Lattanzi, S. Riemer-Sorensen, and J. W. F. Valle, *JCAP* **8**, 013 (2008), arXiv:0805.2372.
- [41] A. Boyarsky, J.-W. den Herder, A. Neronov, and O. Ruchayskiy, *Astroparticle Physics* **28**, 303 (2007), arXiv:astro-ph/0612219.
- [42] A. Boyarsky, D. Iakubovskiy, O. Ruchayskiy, and V. Savchenko, *MNRAS* **387**, 1361 (2008), arXiv:0709.2301.
- [43] S. Riemer-Sorensen and S. H. Hansen, *ArXiv e-prints* (2009), arXiv:0901.2569 [astro-ph.CO].
- [44] A. Boyarsky, A. Neronov, O. Ruchayskiy, and M. Shaposhnikov, *MNRAS* **370**, 213 (2006), arXiv:astro-ph/0512509.
- [45] A. Boyarsky, D. Malyshev, A. Neronov, and O. Ruchayskiy, *MNRAS* **387**, 1345 (2008),

- arXiv:0710.4922.
- [46] H. Yüksel and M. D. Kistler, *Phys. Rev. D* **78**, 023502 (2008), arXiv:0711.2906.
- [47] M. Ackermann, M. Ajello, A. Albert, L. Baldini, G. Barbiellini, K. Bechtol, R. Bellazzini, B. Berenji, R. D. Blandford, E. D. Bloom, E. Bonamente, A. W. Borgland, M. Brigida, R. Buehler, S. Buson, G. A. Calciandro, R. A. Cameron, P. A. Caraveo, J. M. Casandjian, C. Cecchi, E. Charles, A. Chekhtman, J. Chiang, S. Ciprini, R. Claus, J. Cohen-Tanugi, J. Conrad, F. D’Ammando, F. de Palma, C. D. Dermer, E. do Couto e Silva, P. S. Drell, A. Drlica-Wagner, Y. Edmonds, R. Essig, C. Favuzzi, S. J. Fegan, W. B. Focke, Y. Fukazawa, S. Funk, P. Fusco, F. Gargano, D. Gasparrini, S. Germani, N. Giglietto, F. Giordano, M. Giroletti, T. Glanzman, G. Godfrey, I. A. Grenier, S. Guiriec, M. Gustafsson, D. Hadasch, M. Hayashida, D. Horan, R. E. Hughes, T. Kamae, J. Knödlseeder, M. Kuss, J. Lande, A. M. Lionetto, M. Llana Garde, F. Longo, F. Loparco, M. N. Lovellette, P. Lubrano, M. N. Mazziotta, P. F. Michelson, W. Mitthumsiri, T. Mizuno, A. A. Moiseev, C. Monte, M. E. Monzani, A. Morselli, I. V. Moskalenko, S. Murgia, M. Naumann-Godo, J. P. Norris, E. Nuss, T. Ohsugi, A. Okumura, E. Orlando, J. F. Ormes, D. Paneque, J. H. Panetta, M. Pesce-Rollins, F. Piron, G. Pivato, T. A. Porter, D. Prokhorov, S. Rainò, R. Rando, M. Razzano, O. Reimer, M. Roth, C. Sbarra, J. D. Scargle, C. Sgrò, E. J. Siskind, A. Snyder, P. Spinelli, D. J. Suson, H. Takahashi, T. Tanaka, J. G. Thayer, J. B. Thayer, L. Tibaldo, M. Tinivella, D. F. Torres, G. Tosti, E. Troja, J. Vandenbroucke, V. Vasileiou, G. Vianello, V. Vitale, A. P. Waite, B. L. Winer, K. S. Wood, Z. Yang, and S. Zimmer, *Phys. Rev. D* **86**, 022002 (2012), arXiv:1205.2739 [astro-ph.HE].
- [48] D. McCammon, R. Almy, E. Apodaca, W. Bergmann Tiest, W. Cui, S. Deiker, M. Galeazzi, M. Juda, A. Lesser, T. Mihara, J. P. Morgenthaler, W. T. Sanders, J. Zhang, E. Figueroa-Feliciano, R. L. Kelley, S. H. Moseley, R. F. Mushotzky, F. S. Porter, C. K. Stahle, and A. E. Szymkowiak, *Astrophys. J.* **576**, 188 (2002), arXiv:astro-ph/0205012.
- [49] A. Boyarsky, A. Neronov, O. Ruchayskiy, M. Shaposhnikov, and I. Tkachev, *Physical Review Letters* **97**, 261302 (2006), arXiv:astro-ph/0603660.
- [50] S. Riemer-Sørensen, S. H. Hansen, and K. Pedersen, *ApJL* **644**, L33 (2006), arXiv:astro-ph/0603661.
- [51] K. Abazajian and S. M. Koushiappas, *Phys. Rev. D* **74**, 023527 (2006), arXiv:astro-ph/0605271.
- [52] A. Boyarsky, J. Nevalainen, and O. Ruchayskiy, *A&A* **471**, 51 (2007), arXiv:astro-ph/0610961.
- [53] S. Riemer-Sørensen, K. Pedersen, S. H. Hansen, and H. Dahle, *Phys. Rev. D* **76**, 043524 (2007), arXiv:astro-ph/0610034.
- [54] M. Loewenstein, A. Kusenko, and P. L. Biermann, *Astrophys. J.* **700**, 426 (2009), arXiv:0812.2710.
- [55] M. Loewenstein and A. Kusenko, *Astrophys. J.* **714**, 652 (2010), arXiv:0912.0552 [astro-ph.HE].
- [56] A. Boyarsky, O. Ruchayskiy, D. Iakubovskiy, M. G. Walker, S. Riemer-Sørensen, and S. H. Hansen, *MNRAS* **407**, 1188 (2010), arXiv:1001.0644 [astro-ph.CO].
- [57] M. Loewenstein and A. Kusenko, *Astrophys. J.* **751**, 82 (2012), arXiv:1203.5229 [astro-ph.CO].
- [58] E. Borriello, M. Paolillo, G. Miele, G. Longo, and R. Owen, *MNRAS* **425**, 1628 (2012), arXiv:1109.5943 [astro-ph.GA].
- [59] K. Abazajian, G. M. Fuller, and W. H. Tucker, *Astrophys. J.* **562**, 593 (2001), arXiv:astro-ph/0106002.
- [60] C. R. Watson, J. F. Beacom, H. Yüksel, and T. P. Walker, *Phys. Rev. D* **74**, 033009 (2006), arXiv:astro-ph/0605424.
- [61] H. Yüksel, J. F. Beacom, and C. R. Watson, *Physical Review Letters* **101**, 121301 (2008), arXiv:0706.4084.
- [62] C. R. Watson, Z. Li, and N. K. Polley, *JCAP* **3**, 018 (2012), arXiv:1111.4217 [astro-ph.CO].
- [63] D. Forero, M. Tortola, and J. W. F. Valle, *Phys.Rev.* **D86**, 073012 (2012), this updates *New J.Phys.* 13 (2011) 109401 and *New J.Phys.* 13 (2011) 063004 by including the data presented at Neutrino 2012., arXiv:arXiv:1205.4018 [hep-ph].